

CNN-LSTM network-based damage detection approach for copper pipeline using laser ultrasonic scanning

Liuwei Huang^a, Xiaobin Hong^{a,*}, Zhijing Yang^b, Yuan Liu^a, Bin Zhang^a

^a School of Mechanical & Automotive Engineering, South China University of Technology, Guangzhou, Guangdong, PR China

^b School of Information Engineering, Guangdong University of Technology, Guangzhou, Guangdong, PR China



ARTICLE INFO

Keywords:

Laser ultrasonic scanning
Convolutional neural network
Long short-term memory
Deep learning
Copper pipeline
Non-destructive testing

ABSTRACT

Copper pipeline is a commonly used industrial transmission pipeline. Nondestructive testing of copper pipeline early damage is very important. Laser scanning has attracted extensive attention because it can realize the visualization of guided wave propagation and non-contact on-line detection. However, the damage points detection in laser scanning imaging method rely on the difference between the damage points signals and surrounding normal points signals. This limits the applicability of laser scanning and may lead to inaccurate in large-area detection. Facing with such challenges, a damage detection method based on CNN-LSTM network is proposed for laser ultrasonic guided wave scanning detection in this paper, which can detect each scanning point signal without relying on the surrounding detection points signals. Firstly, the proposed data conversion algorithm is used to preprocess the laser scanning signals. Next, CNN-LSTM network is used to train the damage detection model. Four 1D Conv channels with different convolution kernel sizes and depths are designed in Convolutional Neural Network (CNN) module. The module can extract the signal time domain features. Then the features are input into the Long Short-Term Memory Network (LSTM) for feature extraction and classification. Finally, the CNN-LSTM is trained using the laser scanning detection data collected on the copper pipeline with crack and corrosion damages, and applied to detect the copper pipeline damage signal. At the same time, the state-of-the-art methods is compared with proposed method. The experimental results show that the detection accuracy of the method is 99.9%, 99.9%, 99.8% and 99.8% for copper pipeline 0.5 mm deep crack damage, penetrating crack damage, corrosion damage and inside crack damage, respectively. The damage location and size can be accurately detected by the proposed method.

1. Introduction

Copper material has the advantages of high thermal conductivity, good corrosion resistance and easy processing, which makes it a commonly used material for industrial transmission pipeline. Transmission pipeline damage not only affects normal operations, but also wastes resources and threatens the health and safety of operators. Hence, early damage detection is an important issue in the pipeline transportation industry [1,2].

The main damage types of copper pipeline are leak and fracture caused by crack or corrosion. At present, the nondestructive testing technologies for pipeline defects are ultrasonic, dye penetration, magnetic particle testing and eddy current testing etc. [3–6]. However, dye penetrant and magnetic particle testing usually require taking out the tested part for testing, which is not practical for on-line testing. Eddy

current testing cannot detect non-standard surfaces. And the large-scale and quantitative detection of damage can be realized using ultrasonic guided wave testing [7]. The exciting modes of ultrasonic guided wave are electromagnetic ultrasonic, piezoelectric ultrasonic and laser ultrasonic etc. Among them, due to the advantages of non-contact, long working distance, and high sensitivity, laser ultrasonic technology has become an attractive damage detection technology [8–10].

Laser scanning guided wave full wavefield propagation imaging has attracted because it can realize damage visualization [11–15]. Lee Y et al. [16] introduced a rotational scanning method which can achieve high signal-to-noise ratio scanning imaging throughout the cylindrical section of pressure vessels. Toyama et al. [17] used the low-frequency Lamb waves generated by pulsed laser scanning to detect disband in adhesively bonded carbon fiber-reinforced plastics/aluminum joints. Hayashi et al. [18,19] discussed a defect imaging technique using signals

* Corresponding author.

E-mail address: mexbhong@scut.edu.cn (X. Hong).

containing multiple reflected waves. Lee et al. [20] used laser-induced ultrasonic waves to visualize different depth corrosion damage in aluminum alloy plate structures. Wide-band signal is produced by laser ultrasonic excitation, and there are different modes produced by guided wave. Therefore, extract effective features is the key to realize damage detection. Most popular full wavefield signal processing methods rely on various frequency-wavenumber filtering and processing algorithms, which included standing wave separation [21], wigner-ville transform [22] and analysis of the wavenumber-frequency domain [23]. Park et al. [21] used the standing wave filter to separate the standing wave caused by damage, thus realizing the recognition and visualization of hidden damage. Zeng et al. [22] proposed wigner-ville transform ultrasonic propagation imaging method of stronger frequency selectivity. Girolamo et al. [23] used zero-lag cross correlation in the space-frequency domain for damage imaging, and the size quantification and characterization of barely visible impact damage was realized. Kudela et al. [24] by combining the adaptive wave velocity wavenumber domain algorithm with migration learning, it is not necessary to determine the detection frequency. However, these time-frequency domain signal processing methods need to obtain all the signals of full wave field, and some signal information is lost by traditional time-frequency feature extraction method.

Deep learning has been applied in the nondestructive testing field due to its strong ability of feature extraction and feature fusion [25–27]. The deep learning model can be trained to represent high dimensional data, which traditional mathematical model is ill to describe [28–30]. Alguri et al. [31] employed auto-encoder network to reconstruct the full wave field data to reduce the time of full wave field data acquisition. Harley et al. [32–33] realized damage detection without baseline data through dictionary learning and transfer learning. Ebrahimkhanlou et al. [34] applied deep learning methods to localize the acoustic emissions source in the condition of one receive transducer. Hong et al. [35] utilized wavelet transform to catch the waveform features and proposed a liquid level detection method based on autoencoder networks. CNN is one kind of the representative algorithms of deep learning. CNN has the characteristics of local perception and parameter sharing. These two characteristics make CNN can effectively learn the corresponding features from a large number of samples, avoiding the complex feature extraction process. Xu et al. [36] extracted features from the head wave of guided wave signals on multiple monitoring paths, and inputs these features into convolution neural network to identify the length of fatigue crack. Su et al. [37] used the frequency domain characteristics of the signal as the input of CNN to establish the damage classification model. Feng et al. [38] proposed a damage detection method based on image detection and CNN. However, CNN ignores the temporal correlation of vibration signals. LSTM is a recurrent neural network. It can preserve the temporal correlation of vibration signals, which has been applied to vibration signal damage detection. Zhao et al. [39] proposed the early damages detection method based on CNN and LSTM networks, which can detect the breathing crack of cantilever beam. Choe et al. [40] uses LSTM and gated recurrent unit neural networks to detect the structural damage of offshore wind turbine blades, and the high damage detection accuracy is realized. The damage detection accuracy can be optimized using the time series characteristics obtained by SLTM, which is illustrated by the above literature.

In the traditional laser scanning detection, the damage points detection in laser scanning imaging method rely on the difference between the damage points signals and surrounding normal points signals. There may be false detection during large-area detection. Whether there are damage points can be judged only after complete scanning the detection area. At present, the Structure Health Monitoring (SHM) technologies are developed towards automation, intelligence and reducing expert dependence. In this paper, CNN-LSTM network is used to mine the features of laser signal and detect each scanning point. In this way, the false detection rate of large-scale scanning detection is reduced, and the applicability of laser scanning detection method can be

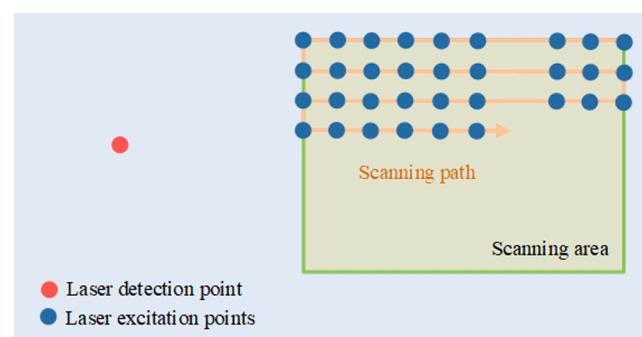


Fig. 1. Principle diagram of laser scanning damage imaging.

improved. However, classical CNN feature extraction ignores the time domain characteristics of signals. Four 1D Conv channels with different convolution kernel sizes and depths are designed. The convolution layers retain the signal timing features. Then the features are input into the LSTM for feature extraction and classification. At the same time, the damage detection accuracy is affected by the vibration time difference of different positions scanning points, which is eliminated by the designed data conversion algorithm.

This paper is organized as follows. **Section 2** introduces the theoretical background and the procedure of proposed method. In **Section 3**, experiments are carried out. The effectiveness of the proposed method is verified by the copper pipeline damage detection data. The state-of-the-art methods is compared with the proposed method. Finally, **Section 4** comes to the conclusions.

2. Damage detection method for copper pipeline

The traditional laser ultrasonic scanning damage detection methods mostly rely on the signal difference between the damage point and the normal points. However, the whole detection area is needed to scanning before damage detection by these methods, which is easy to inaccurate detection when detecting large-area damage. These shortcomings limit the application of laser scanning detection method. To identify the damage, it is necessary to obtain the accurate characteristic signal information, especially the difference of the normal points and the damage points signal. Deep learning has good performance in the feature extraction and processing of data. In this section, a laser ultrasonic signal detection method based on CNN-SLTN network is introduced, which used to detect the laser scanning signal.

2.1. Data preprocessing based on data conversion algorithm

Laser ultrasonic imaging technology can realize the damage visual detection. In the process of laser scanning, one scanning method is to fix the detection point and move the excitation point, another method is to fix the excitation point and move the detection point. The pipeline is a curved surface structure, which is suitable for the first scanning method. The schematic diagram of laser scanning imaging technology is shown in Fig. 1. There are two ways, thermoelastic mechanism and ablation mechanism, to excite ultrasound by pulsed laser [41]. Since the laser has no damage to the material surface under the thermoelastic mechanism, the thermoelastic mechanism is more suitable for the field of non-destructive testing. However, the signal produced by laser thermoelastic mechanism is weak. And the detection signals of different position are quite different due to the radian and excited position of the pipeline. Therefore, signal preprocessing is needed before feature extraction. Next, the data conversion algorithm is introduced.

Due to the weak laser signal and the low signal-to-noise ratio, the signal is collected multiple times at each scanning point. The number of length and width direction scanning points in the detection rectangular area is M and N respectively, the number of vibration signal sampling

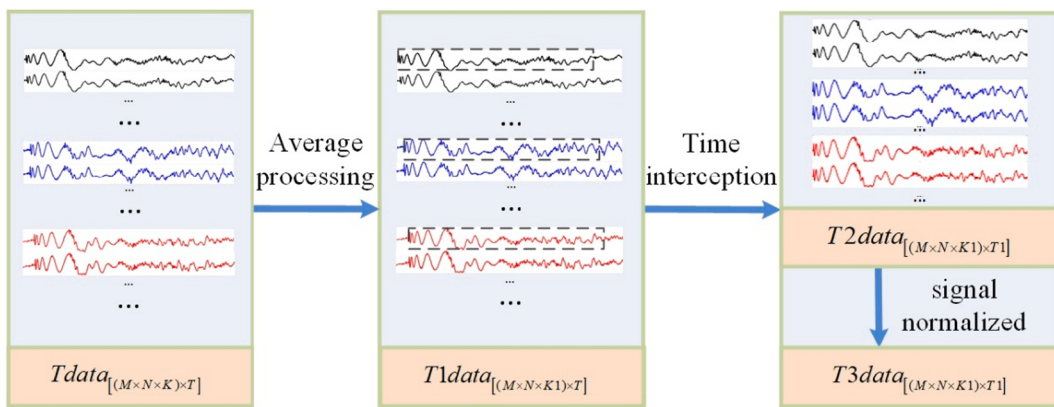


Fig. 2. Laser ultrasonic testing signal preprocessing flow chart.

points is T , and the number of each excitation acquisition point is K . In this way, the original time domain signal matrix $Tdata_{[(M \times N \times K) \times T]}$ of the two-dimensional detection area is obtained. Training deep learning model requires a large number of samples. If the samples of each point need to average many times, a large number of original signals are required. To overcome this problem, a large number of samples are obtained by randomly selecting several times averages from a group of signals. After averaging, a new time domain signal matrix $T1data_{[(M \times N \times K1) \times T]}$ can be obtained. In the detection area, the accuracy of damage identification will be reduced due to the time difference of signals at different positions. Therefore, the signal is saved from the

beginning of vibration, then the signal matrix $T2data_{[(M \times N \times K1) \times T1]}$ with shorter sampling points is obtained. Next, the signal is normalized and the new matrix $T3data_{[(M \times N \times K1) \times T1]}$ is obtained. And each sample is marked through the label set $Labeltrain_{[(M \times N \times K1) \times 1]}$. Finally, the data is imported into the model for detection. The laser ultrasonic detection preprocessing is shown in Fig. 2.

Next, the steps of data preprocessing are introduced. The average processing for the p ($p = 1, 2, \dots, M \times N$) point signal is as follows. The matrix $Tdata_{[K \times T]}$ of the point p is extracted from the time-domain signal matrix $Tdata_{[(M \times N \times K) \times T]}$ (Eq. (1)). The numbers from 1 to K are randomly sorted and the first m signals are averaged to get one sample

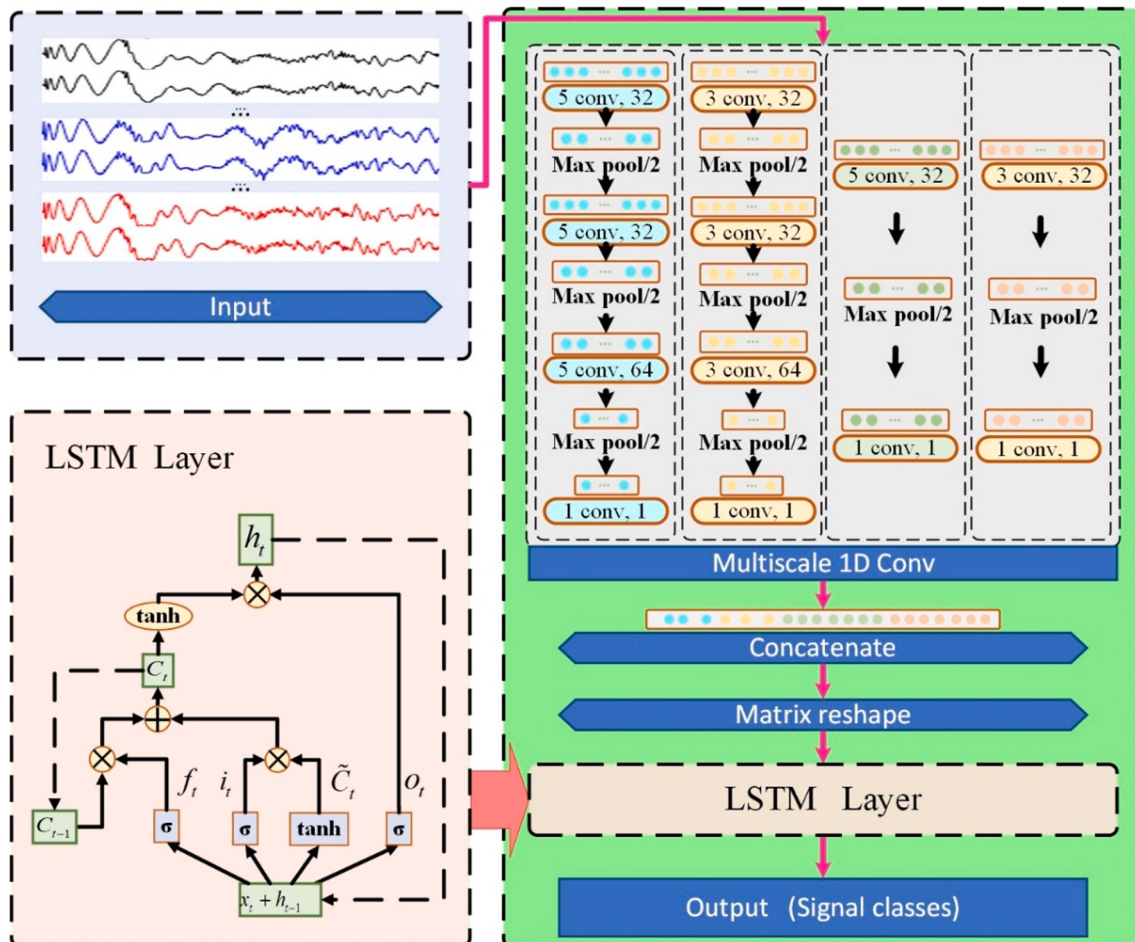


Fig. 3. CNN-LSTM network structure diagram.

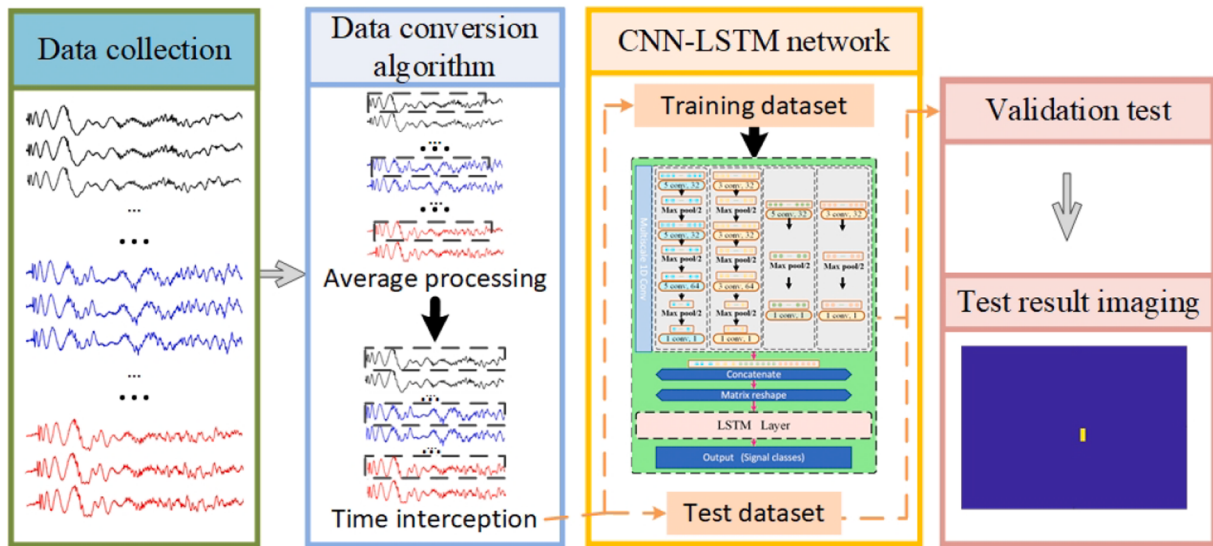


Fig. 4. Flowchart of CNN-LSTM-based nondestructive damage detection procedure.

(Eq. (2)). Repeat this step $K1$ times to get $K1$ samples. The value of $K1$ is determined by the samples required to establish CNN-LSTM network.

$$Tedata = (Tdata_{(p-1) \times k+1}; Tdata_{(p-1) \times k+2}; \dots; Tdata_{p \times k}) \quad (1)$$

$$Te^j = Rsort(1, 2, \dots, K), T1data_{(p-1) \times k1+j} = \sum_{i=Td_1^j}^{Td_m} Tedata_i / m(j \\ = 1, 2, \dots, K1) \quad (2)$$

where the function $Rsort()$ represents a random sorting of numbers. Since the signals of different positions in the scanning area are trained in the CNN-LSTM network, it is necessary to eliminate the influence of excitation position on the detection signal. The vibration starting time of different points in the scanning area is not consistent, so it is necessary to adjust the starting time of the signal. The vibration signal is adjusted to save from the beginning of vibration. To eliminate the interference of noise, the first extreme point greater than the average value of vibration signal is found, and the position of the first 15 extreme points is taken as the vibration starting point. There are about 1–2 μ s from the beginning of vibration to the first extreme position, and the sampling rate is 5 MHz. Therefore, the vibration signals are saved from 15 points before the first extreme position. And save the next $T1$ length signals. The value of $T1$ is determined by the length of time required to the signal. In this way, a new time domain signal matrix $T2data_{[(M \times N \times K1) \times T1]}$ can be obtained. Then, data normalization is realized to reduce the statistical difference of different samples. In this step, zero mean normalization is used. For vibration signal $T2data_q$ ($q = 1, 2, \dots, M \times N \times K1$), the calculation of the zero mean normalization can be described as follows

$$T3data_q^j = \frac{T2data_q^j - \overline{T2data}_q}{S_{T2data_q}}, (j = 1, 2, \dots, T1) \quad (3)$$

where $T3data_q^j$ is the j^{th} element of the normalized signal, $T2data_q^j$ is the j^{th} element of the original signal, $\overline{T2data}_q$ is the mean value of the original signal, and S_{T2data_q} is the standard deviation of the original signal. After normalization, the matrix $T3data_{[(M \times N \times K1) \times T1]}$ is obtained. The training label $Labeltrain_{[(M \times N \times K1) \times 1]}$ is obtained according to whether each matrix corresponding sample is normal or damaged. The label of the normal sample is 0, and the label of the damaged sample is 1. Next, input the data into the CNN-LSTM network for training.

2.2. Damage detection method based on CNN-LSTM network

The CNN-LSTM network consists of CNN module and LSTM layer. The structural diagram of CNN-LSTM network is shown in Fig. 3. In CNN module, data is input to four convolution channels. Among them, two channels have one-layer convolution, and the convolution kernel sizes are 3 and 5 respectively. Another two channels have three-layer convolution, and the convolution kernel sizes are 3 and 5 respectively. The convolution kernel of the last convolution layer in each channel is 1. Through the multi-scale 1D convolution feature extraction, the signal features can be deeply mine and each channel output features maintain the original signal time domain characteristics. Then the four channels features are connected for matrix transformation. Next, the features are input into LSTM layer to further extract features.

LSTM layer is cyclic layer structure, which can extract the time domain characteristics of signals. The first step in LSTM is to select the initial cell state information to throw away. This decision is made by the forget gate. It looks at h_{t-1} and x_t , and outputs a number between 0 and 1 for each number in the cell state C_{t-1} .

$$f_t = \sigma(W_f \cdot [h_{t-1}, x_t] + b_f) \quad (4)$$

where W_f and b_f represent the weight matrix and offset value of the forget gate, respectively. $[h_{t-1}, x_t]$ represents connecting two vectors into one. In next step, the new cell state information is selected to store. The input gate decides which values will update. Then, a Tanh layer creates a vector of new candidate values \tilde{C}_t , which could be added to the state. Next, these two are combined to create an update state.

$$i_t = \sigma(W_i \cdot [h_{t-1}, x_t] + b_i) \quad (5)$$

$$\tilde{C}_t = \tanh(W_C \cdot [h_{t-1}, x_t] + b_C) \quad (6)$$

where W_i and b_i represent the weight matrix and offset value of the input gate, respectively. W_C and b_C represent the weight matrix and offset value of the cell status, respectively. The old cell state C_{t-1} is update into the new cell state C_t . This is a step to delete the old subject gender information and add new information.

$$C_t = f_t * C_{t-1} + i_t * \tilde{C}_t \quad (7)$$

Next, the output information is needed to decided. This output is based on cell state, but it is filtered version. A sigmoid layer is running to decide what parts of the cell state are going to output. The cell state is put through tanh and multiply it by the output of the sigmoid gate.

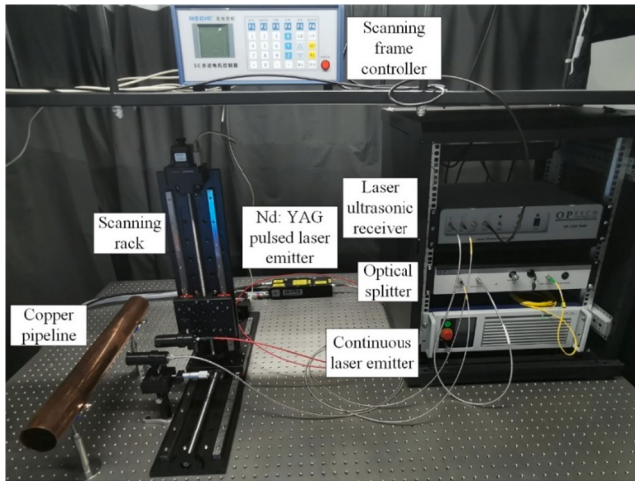


Fig. 5. Experimental setup diagram for defects detection in copper pipeline.

$$o_t = \sigma(W_o \cdot [h_{t-1}, x_t] + b_o) \quad (8)$$

$$h_t = o_t * \tanh(C_t) \quad (9)$$

where W_o and b_o represent the weight matrix and offset value of the output gate, respectively.

In the LSTM layer, features with timing information can be obtained due to x_t repeated input and update. After passing through the LSTM layer, the output h_t can be obtained. Then it is classified by softmax layer. According to the difference between each sample output and the label value, the parameters in the model are adjusted. The loss function is given as follows

$$\text{loss} = \frac{1}{2} \sum_{k=1}^R (t_k - y_k)^2 \quad (10)$$

where R denotes the number of responses, t_k signifies the target output and y_k is the prediction for the response k . The laser ultrasonic signal damage detection model is obtained by training data. After obtaining the

laser ultrasonic damage detection model, the laser ultrasonic scanning testing data can be input into the model, and the test results can be obtained. Then the signal sample label values are averaged, and the excitation point is determined as damage or not according to the averaged label value. The sample is marked as normal when its label value is less than 0.5. Otherwise, it is marked as damage sample. Finally, all the label values are converted into two-dimensional matrix for imaging to realize the visualization of damage detection. The process of the proposed method is shown in Fig. 4. In next section, the effectiveness is verified by the copper pipeline laser scanning experiment.

3. Experimental and discussion

3.1. Experimental process

In this section, the damage detection effect of the proposed method is verified by the copper pipeline laser scanning data. To verify the detection ability of network model, the surface and internal damage that often appear in the copper pipeline are detected. The copper pipeline damage detection experimental system based on laser ultrasonic testing equipment is established. The experimental system is shown in Fig. 5, including Q-switched 1064 nm Nd:YAG pulsed laser emitter, laser ultrasonic signal receiving system. To avoid damaging the pipeline, the laser excitation is thermoelastic mechanism. The Q-switched 1064 nm Nd: YAG pulse laser transmitter emission pulse value is 10 ns, the energy is 30 mJ, and the spot diameter is 1 mm. The AIR-1550-TWM laser ultrasonic testing system is used to detect the surface displacements of the detect points. The sampling rate is 5 MHz. The signal received by the laser detection system is saved by the data acquisition card, then processed in the computer. The sampling time is 600 μ s.

The copper pipeline with size of 500 mm \times Φ 65mm \times 2 mm is used in the experiment. To verify the detection capability of the established model, the crack damages and corrosion damage are tested in this experiment. There are 0.5 mm deep crack damage, penetrating crack damage, corrosion damage and inside crack damage. The damage size of 0.5 mm deep crack is 0.5 mm \times 0.5 mm \times 3 mm, the penetrating crack size is 0.5 mm \times 3 mm, the corrosion area is about 14 mm \times 14 mm and inside crack damage size is about 0.6 mm \times 1 mm \times 16 mm. The damaged copper pipelines are shown in Fig. 6. The square area on the

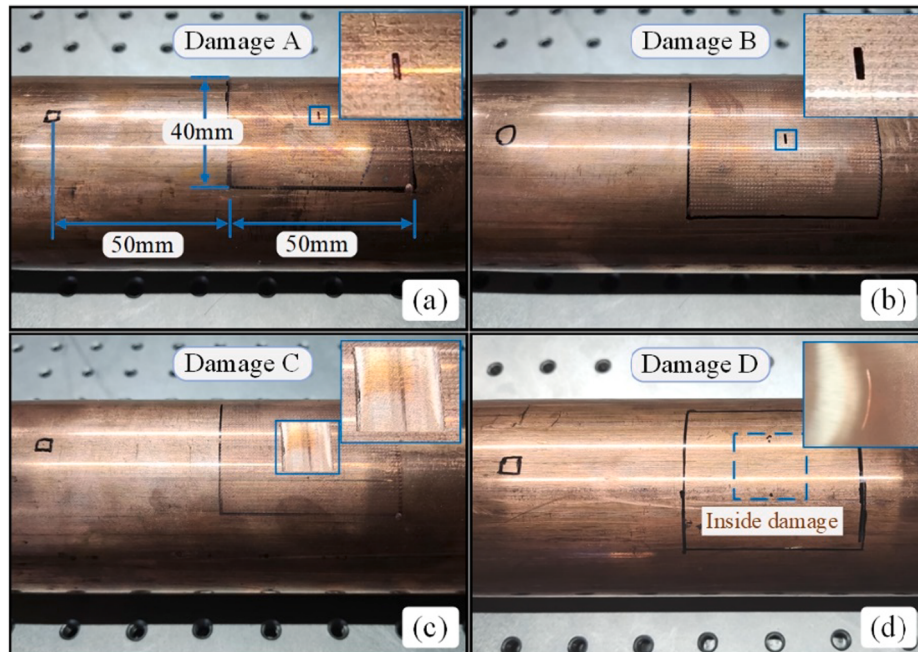


Fig. 6. The picture of copper pipeline with (a) 0.5 mm deep crack damage, (b) penetrating crack damage, (c) corrosion damage and (d) inside crack damage.

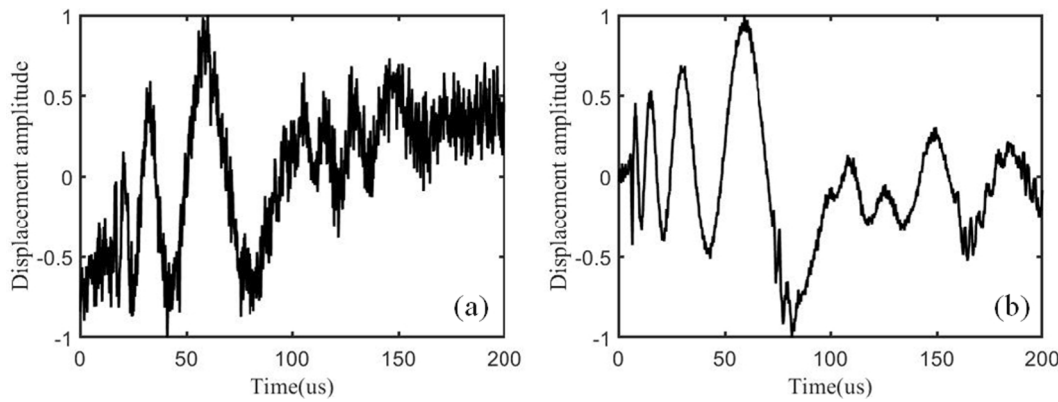


Fig. 7. (a) Original time domain signal, (b) average processed time domain signal.

right is the scanning area, and the position drawn on the left is the detection point. The shortest distance between the detection point and the scanning area is 50 mm.

In the experiment, the position of laser excitation points is controlled by the scanning rack, and the distance between adjacent excitation points is 1 mm. The amplitude of single acquisition signal is low and the signal-to-noise ratio is low. Signal are collected 50 times at each excitation point for signal preprocessing. After scanning, the time-domain signal matrix $T_{data}[(4 \times 40 \times 50) \times 6000 \times 50]$ is obtained, in which 4 represents four types of damage, 40 and 50 are the excitation points in the length and width direction of the detection rectangular area, 6000 represents the signal length at each point and 50 is the acquisition times of each excitation point position. The original time domain signal of a random point is show in Fig. 7(a). The signal-to-noise ratio of time-domain signals is improved by randomly selecting 40 signals for average from 50 signals. And the obtained wave is shown in Fig. 7(b).

After averaging the original time domain signals, total 8000 samples are obtained from one kind damage pipeline laser scanning experiment, which including 4000 normal samples and 4000 damaged samples. Among them, 2000 damaged samples are reserved for each damaged pipeline scanning data, and 2000 normal samples are used for training. The others are for testing. To enhance the generalization ability of detection model, the four groups experimental data are uniformly labeled for training and damage identification. The categories of labels are normal and damage. The total number of training samples is 16000, including 8000 damaged samples and 8000 normal samples. In the proposed method, there are many parameters and functions. Next, determine the values of these parameters.

Table 1

Training data detection accuracy by different data conversion algorithm parameters.

m	35	40	45
Verification set detection accuracy	0.963	0.976	0.970
T_1	1200	2400	3600
Verification set detection accuracy	0.963	0.977	0.973

3.2. Experimental parameters analysis

3.2.1. Data conversion algorithm parameter analysis

In data conversion algorithm, there are some flexibly setting parameters, such as the number of original samples K collected at each scanning point, the number of original samples m required to calculate the average signal at each time, the number of stable signal samples K_1 after average at each scanning point, and the time length T_1 after the starting point of interception time. The acquisition time of training signal is affected by the number of original samples K , which does not affect the detection speed of the model. Since there are 2000 scanning points in the detection area, the number of stable sample signals K_1 is sufficient. Therefore, signals number m used to calculate the average and the signal time length T_1 are discussed. The 80% of the training data are randomly selected for training set and the remaining 20% are set as verification set. The identification accuracy of the verification set is used to judge whether the model parameters are appropriate.

The similarity of model data is affected by signals number m used to calculate the average. The signal-to-noise ratio will decrease due to the decrease of m value. Increasing the value of m will improve the similarity of the signal, but the generalization ability of the detection model will be reduced. Here, m is set as 35, 40 and 45 respectively to compare the fitting results of data to the model. The detection model testing time is

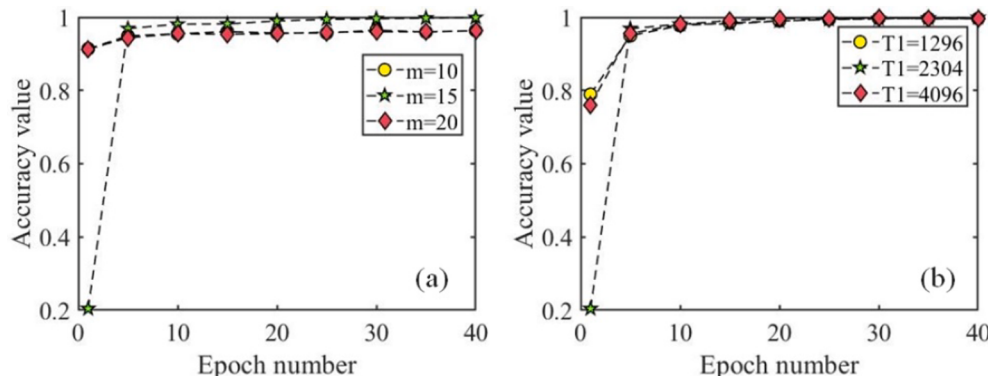


Fig. 8. Accuracy of (a) different optimization algorithms and (b) different activation functions.

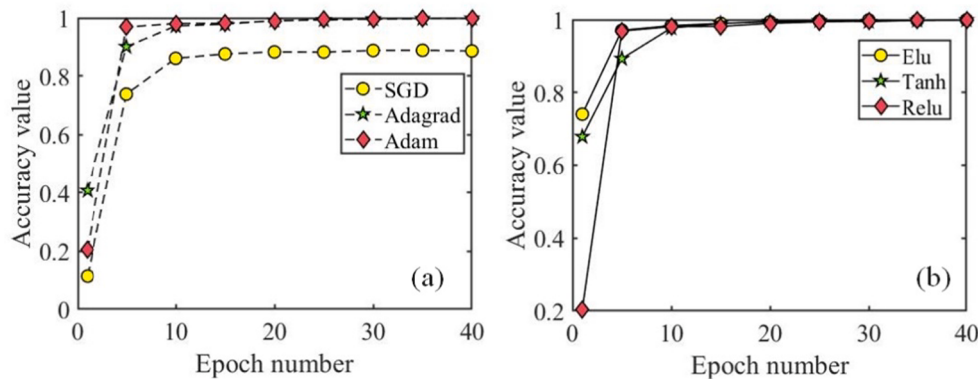


Fig. 9. Accuracy of (a) different optimization algorithms and (b) different activation functions.

Table 2

Training data detection accuracy by different optimizers and activation functions.

Optimizer	Adam	RMSprop	SGD
Verification set detection accuracy	0.978	0.974	0.931
Activation	Relu	Tanh	Elu
Verification set detection accuracy	0.978	0.976	0.976

affected by the signal length T_1 . The testing time of detection model will increase with the increase of signal length. However, the effective characteristics of the signal will be lost when the signal length is too short. Here, T_1 is set to 1200, 2400 and 3600 respectively to compare the detection results. The model convergence speed with different data conversion algorithm parameters is shown in Fig. 8.

From Fig. 8, different values of m and T_1 have little effect on the convergence rate. The training data detection accuracy using different data conversion algorithm parameters are shown in Table 1. From Table 1, the highest detection accuracy is obtained when m is equal to 40. The noise of the signal may increase when m is equal to 35. And the consistency of the signal is too high when m is equal to 45. For different T_1 value, the fitting effect of the data on the model is the lowest when the time length T_1 is equal to 1200. The detection accuracy obtained by T_1 is equal to 2400 and 3600 are similar. Therefore, the time length T_1 equal to 2400 is the best choice, because the computing time is reduced using shorter data length.

3.2.2. CNN-LSTM network functions analysis

Next, different optimizers and activation functions are used for comparison. The function of the optimizer is to optimize the parameters of the network model. Stochastic Gradient Descent (SGD), Adam and Adaptive Gradient Algorithm (Adagrad) are commonly used optimizers. Next, SGD, Adagrad and Adam optimization algorithms are compared. The activation function introduces non-linear factor to the network. This allows neural networks to be applied to non-linear problems, not just linear problems. For activation function, the RELU, ELU and Tanh are used to comparison. There calculation formulas are shown in Eq. (11), Eq. (12) and Eq. (13). The model convergence speed with different optimizers and activation functions is shown in Fig. 9.

$$f(x) = \max(0, x) \quad (11)$$

$$f(x) = \begin{cases} \alpha(e^x - 1), & x \leq 0 \\ x, & x > 0 \end{cases} \quad (12)$$

$$f(x) = \frac{e^x - e^{-x}}{e^x + e^{-x}} \quad (13)$$

From Fig. 9(a), SGD converges slowly, and both Adagrad and Adam are converged quickly. Different activation functions have little effect on

Table 3

Damage detection accuracy of different methods.

Detection methods	LeNet5	ResNet	CNN-LSTM
Damage A (0.5 mm deep crack damage)	0.954	0.971	0.999
Damage B (penetrating crack damage)	0.975	0.984	0.998
Damage C (corrosion damage)	0.941	0.952	0.998
Damage D (inside crack damage)	0.989	0.992	0.998

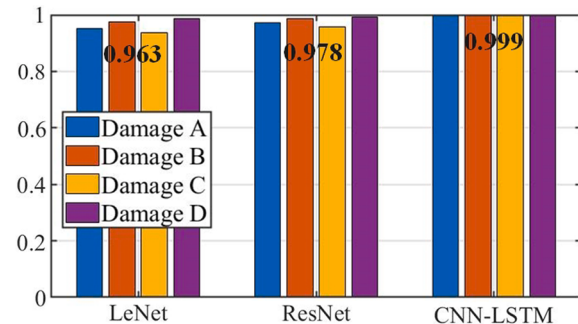


Fig. 10. Damage detection accuracy of three methods.

the convergence rate of the model. Their verification set test accuracy is shown in Table 2.

The detection effect of the verification set is shown in Table 2. Among different optimizers, Adam has the highest detection accuracy. The detection accuracy of different activation functions is similar, and Relu is slightly higher. Therefore, Adam is selected as the optimizer and Relu is selected as the activation.

After determining the parameters of the propose method, the training data is imported into CNN-LSTM network to get the laser ultrasonic damage detection model. The damage identification results of 0.5 mm deep crack damage, penetrating crack damage, corrosion damage and inside crack damage pipeline are introduced in next section. To illustrate the detection effect of the proposed method, the state-of-the-art methods is compared with proposed method.

3.3. Results and discussion

3.3.1. Experimental results comparisons with state-of-the-art methods

To evaluate the detection performance of CNN-LSTM network, LeNet5 and ResNet networks are used for comparison. The LeNet5 is a classical convolutional neural network, which has been applied in various fields [42]. The ResNet is easier to capture the subtle fluctuations of identity mapping than ordinary mapping [43]. In the ResNet block, the input data can be transmitted forward faster through cross layer data lines. The network parameter settings of the two comparison

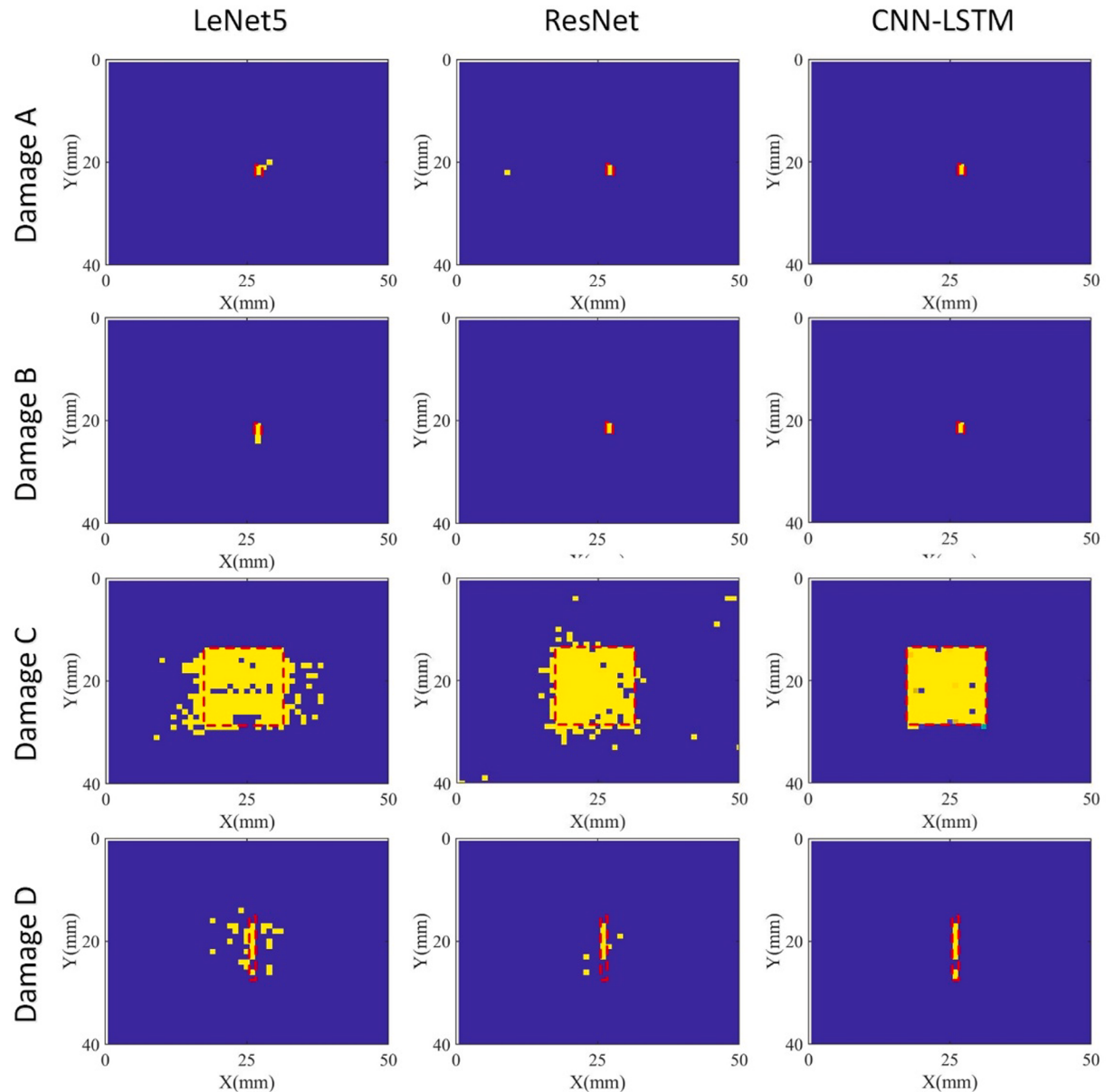


Fig. 11. Imaging results of four kinds damage.

methods are the same as proposed method. The detection results of these networks are shown in Table 3.

From Table 3, the detection accuracy of the four kinds of damage is more than 0.95. Comparing the detection accuracy of different damage, the three methods have the lowest detection accuracy of corrosion damage. The average detection accuracy of internal damage exceeds 0.99. The detection results histogram of the three methods is shown in Fig. 10. The average accuracy value of the three damage detection results by proposed methods is higher than commonly used CNN.

Network structure is the main difference between LeNet5, ResNet and CNN-LSTM. The signal time domain characteristics is retained proposed CNN-LSTM method. Results show that more accurate detection results are obtained by retaining the signal time domain characteristics.

After the test results are obtained, the test sample is converted to the scanning position for damage imaging. The imaging result is shown in Fig. 11. In the figure, yellow points mean the detection result is damage, and blue points mean the detection result is normal. The actual damage location is indicated by a red dashed box. From Fig. 11, the detection

accuracy of different types damage is quite different. Comparing 0.5 mm deep crack damage with penetrating crack damage, because 0.5 mm deep crack damage is not through damage, damage detection is relatively difficult. Both LeNet5 and ResNet have detected errors. And high penetrating crack damage detection accuracy is achieved by all three methods. Due to the large corrosion damage area and inconsistent defect depth, the three methods detect result is inaccurate. Because the reflected signal of internal damage is weak, the detection results also be inaccurate. Compared with the traditional CNN, proposed CNN-LSTM network which retains the time domain characteristics has better detection result in all four kinds damage.

3.3.2. Multi-location damage detection

In this work, the damage location of the signal to be detected is the same as training model signal. In theory, damage detection can be realized as long as the damage signals in the detection area. To verify the robustness of this method, the original detection model is used to detect the damage at different locations in this section. The damage location is shown in Fig. 13.

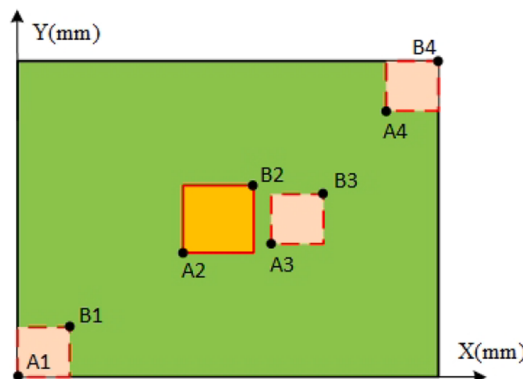


Fig. 12. Supplementary damage locations.

The solid-line square area in Fig. 12 is the original experimental damage location, and the three dashed-line square areas are the three supplementary damage location. For the 0.5 mm deep crack damage and penetrating crack damage, the coordinates of each point are A1(4, 4), B1 (4, 5), A2(25, 20), B2(25, 21), A3(29, 20), B3(29, 21), A4(44, 34), B4 (44, 35). For the corrosion damage pipeline detection area, the coordinates of the points in the figure are A1(0, 0), B1(7, 7), A2(17, 12), B2 (30, 25), A3(32, 17), B3(39, 24), A4(42, 32), B4(49, 39). For the inside crack damage, the coordinates of each point are A1(6, 4), B1(6, 19), A2 (26, 14), B2(26, 29), A3(30, 15), B3(30, 30), A4(45, 16), B4(45, 35). The supplementary samples are all damaged samples, 600 samples for each damage and 200 samples for each location. Among them, 0–200 samples are in the lower left region, 201–400 samples are in the middle region, and 401–600 samples are in the upper right region. The damage samples in the training data is only the original location damage. The detection results are shown in Fig. 13.

The detection accuracy rates of 0.5 mm deep crack damage, penetrating crack damage, corrosion damage and inside crack damage are 100%, 100%, 79.3% and 85.8%, respectively.

Among them, cracks damage has achieved high detection accuracy, and the detection accuracy of corrosion damage is low. At the same time,

the damage detection accuracy in the middle area is higher than that in the other two locations. This shows that the detection accuracy is affected by damage location. The damage detection accuracy should be improved by adding damage signals at different locations.

4. Conclusions

To achieve high-precision damage detection of copper pipelines, a damage detection method based on CNN-LSTM network is applied to laser ultrasonic scanning signals detection. Firstly, the data conversion algorithm is used to preprocess the detect signal. Then, the data is input into the CNN-LSTM network to train the detection model. Finally, the copper pipelines with 0.5 mm deep crack damage, through crack damage, corrosion damage and inside damage are detected and imaged.

The results show that the proposed method can realize accurate visual damage detection of copper pipeline. The advantages of this work are as follows. (1) Proposed method can detect the damage of a single scanning point without relying on the signals of the surrounding detection points. Rapid and accurate damage identification are realized. The applicability of laser scanning detection method is improved by proposed CNN-LSTM network. (2) The time domain characteristics of laser detection signals is preserved by proposed method, which is improve the damage detection accuracy. However, the detection accuracy is affected by the damage location. In the future research, the robustness of deep learning method in laser scanning multi damage detection will be studied.

Funding

This work is supported in part by the National Natural Science Foundation of China under Grant 51975220, in part by the Guangdong Province Science and Technology Project under Grant 2019B010154002 and 2020B0404010001, in part by the Guangdong Outstanding Youth Fund under Grant 2019B151502057, and in part by the Fundamental Research Funds for Central Universities project under Grant 2019ZD23.

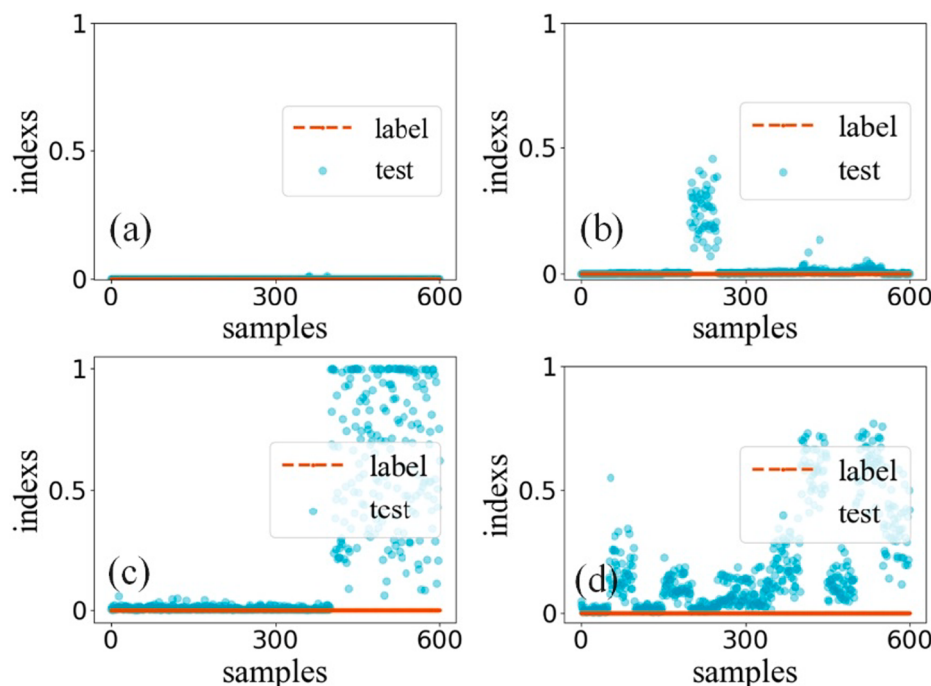


Fig. 13. Multi-location (a) 0.5 mm deep crack damage, (b) penetrating crack damage, (c) corrosion damage and (d) inside crack damage.

Declaration of Competing Interest

The authors declare that they have no known competing financial interests or personal relationships that could have appeared to influence the work reported in this paper.

References

- [1] X. Hong, Y. Liu, X. Lin, Z. Luo, Z. He, Nonlinear ultrasonic detection method for delamination damage of lined anti-corrosion pipes using PZT transducers, *Appl. Sci.* 8 (11) (2018) 2240, <https://doi.org/10.3390/app8112240>.
- [2] B. Zhang, S. Zhang, W. Li, Bearing performance degradation assessment using long short-term memory recurrent network, *Comput. Ind.* 106 (2019) 14–29.
- [3] W. Xu, C. Yang, H. Yu, et al., Microcrack healing in non-ferrous metal tubes through eddy current pulse treatment, *Sci. Rep.* 8 (2018) 6016.
- [4] P. Liu, A.W. Nazirah, H. Sohn, Numerical simulation of damage detection using laser-generated ultrasound, *Ultrasonics* 69 (2016) 248–258.
- [5] Y. Liu, Z. Lian, T. Lin, et al., A study on axial cracking failure of drill pipe body, *Eng. Fail. Anal.* 59 (2016) 434–443.
- [6] B. Dong, G. Fang, Y. Liu, et al., Monitoring reinforcement corrosion and corrosion-induced cracking by X-ray microcomputed tomography method, *Cem. Concr. Res.* 100 (2017) 311–321.
- [7] S. Fateri, P.S. Lowe, B. Engineer, N.V. Boulgouris, Investigation of ultrasonic guided waves interacting with piezoelectric transducers, *IEEE Sens. J.* 15 (8) (2015) 4319–4328.
- [8] Y. Watanabe, A. Yonezu, X. Chen, Measurement of interfacial fracture toughness of surface coatings using pulsed-laser-induced ultrasonic waves, *J. Nondestr. Eval.* 37 (1) (2018) 2.
- [9] T. Hayashi, M. Murase, N. Ogura, T. Kitayama, Imaging defects in a plate with full non-contact scanning laser source technique, *Mater. Trans.* 55 (7) (2014) 1045–1050.
- [10] W. Zeng, H. Wang, G. Tian, W. Wang, Detection of surface defects for longitudinal acoustic waves by a laser ultrasonic imaging technique, *Optik-Int. J. Light Electron Opt.* 127 (1) (2016) 415–419.
- [11] M. Chen, Q. Huan, Z. Su, et al., A tunable bidirectional SH wave transducer based on antiparallel thickness-shear (d15) piezoelectric strips, *Ultrasonics* 98 (3) (2019) 5–50.
- [12] A. Kromine, P. Fomitchov, S. Krishnaswamy, et al., Applications of scanning laser source technique for detection of surface-breaking defects, *Opt. Diagnost. Ind. Appl.* 4076 (2000) 252–259.
- [13] B.S. Marcio, P. Nienheysen, D. Habor, et al., Quality assessment and deviation analysis of three-dimensional geometrical characterization of a metal pipeline by pulse-echo ultrasonic and laser scanning techniques, *Measurement* 145 (2019) 30–37.
- [14] H.-J. Shin, J.-R. Lee, Development of a long-range multi-area scanning ultrasonic propagation imaging system built into a hangar and its application on an actual aircraft, *Struct. Health Monit.-An Int. J.* 16 (1) (2017) 97–111.
- [15] P. Liu, H. Sohn, B. Park, Baseline-free damage visualization using noncontact laser nonlinear ultrasonics and state space geometrical changes, *Smart Mater. Struct.* 24 (6) (2015) 065036, <https://doi.org/10.1088/0964-1726/24/6/065036>.
- [16] Y. Lee, H. Ahmed, J. Lee, Filament-wound composite pressure vessel inspection based on rotational through-transmission laser ultrasonic propagation imaging, *Compos. Struct.* 236 (2020), 111871.
- [17] N. Toyama, T. Yamamoto, K. Urabe, H. Tsuda, Ultrasonic inspection of adhesively bonded CFRP/aluminum joints using pulsed laser scanning, *Adv. Compos. Mater* 28 (1) (2019) 27–35.
- [18] T. Hayashi, Imaging defects in a plate with complex geometries, *Appl. Phys. Lett.* 108 (8) (2016) 081901, <https://doi.org/10.1063/1.4942599>.
- [19] H. Takahiro, High-speed non-contact defect imaging for a plate-like structure, *NDT E Int.* 85 (2017) 53–62.
- [20] I. Lee, A. Zhang, C. Lee, S. Park, A Visualization method for corrosion damage on aluminum plates using an Nd:YAG pulsed laser scanning system, *Sensor.* 16 (12) (2016) 2150, <https://doi.org/10.3390/s16122150>.
- [21] B. Park, Y. An, H. Sohn, Visualization of hidden delamination and debonding in composites through noncontact laser ultrasonic scanning, *Compos. Sci. Technol.* 100 (2014) 10–18.
- [22] W. Zeng, H. Wang, G. Tian, et al., Application of laser ultrasound imaging technology in the frequency domain based on Wigner-Ville algorithm for detecting defect, *Opt. Laser Technol.* 74 (2015) 72–78.
- [23] D. Girolamo, H. Chang, F. Yuan, Impact damage visualization in a honeycomb composite panel through laser inspection using zero-lag cross-correlation imaging condition, *Ultrasonics* 87 (2018) 152–165.
- [24] P. Kudela, M. Radzinski, W. Ostachowicz, Impact induced damage assessment by means of Lamb wave image processing, *Mech. Syst. Sig. Process.* 102 (2018) 23–36.
- [25] H. Liu, Y. Zhang, Deep learning based crack damage detection technique for thin plate structures using guided lamb wave signals, *Smart Mater. Struct.* 29 (1) (2020) 015032, <https://doi.org/10.1088/1361-665X/ab58d6>.
- [26] E.F.S. Filho, M.M. Silva, P.C.M.A. Farias, et al., Flexible decision support system for ultrasound evaluation of fiber-metal laminates implemented in a DSP, *NDT & E Int.: Ind. Nondestructive Test. Evaluat.* 79 (2016) 38–45.
- [27] K. Li, Z. Ma, P. Fu, S. Krishnaswamy, Quantitative evaluation of surface crack depth with a scanning laser source based on particle swarm optimization-neural network, *NDT and E Int.* 98 (2018) 208–214.
- [28] N. Toyama, J. Ye, W. Kokuyama, S. Yashiro, Non-contact ultrasonic inspection of impact damage in composite laminates by visualization of lamb wave propagation, *Appl. Sci.* 9 (1) (2018) 46, <https://doi.org/10.3390/app9010046>.
- [29] H. Song, Y. Yang, Noncontact super-resolution guided wave array imaging of subwavelength defects using a multiscale deep learning approach, *Struct. Health Monit.* 20 (4) (2021) 1904–1923.
- [30] R. Zhao, R. Yan, Deep learning and its applications to machine health monitoring, *Mech. Syst. Sig. Process.* 115 (2019) 213–237.
- [31] K.S. Alguri, J.B. Harley, Transfer learning of ultrasonic guided waves using autoencoders: a preliminary study, *AIP Conf. Proc.* 2102 (1) (2019), 050013.
- [32] K.S. Alguri, C.C. Chen, J.B. Harley, Sim-to-real: employing ultrasonic guided wave digital surrogates and transfer learning for damage visualization, *Ultrasonics* 111 (1851) (2021), 106338.
- [33] K.S. Alguri, J. Melville, J.B. Harley, Baseline-free guided wave damage detection with surrogate data and dictionary learning, *J. Acoust. Soc. Am.* 143 (6) (2018) 3807–3818.
- [34] A. Ebrahimkhanlou, S. Salamone, Single-sensor acoustic emission source localization in plate-like structures using deep learning, *Aerospace.* 5 (2) (2018) 50.
- [35] X. Hong, B. Zhang, Y. Liu, Liquid level detection in porcelain bushing type terminals using piezoelectric transducers based on auto-encoder networks, *Measurement* 141 (2019) 12–23.
- [36] L. Xu, S. Yuan, J. Chen, et al., Guided wave-convolutional neural network based fatigue crack diagnosis of aircraft structures, *Sensors.* 19 (16) (2019) 3567.
- [37] C. Su, M. Jiang, S. Lv, S. Lu, L. Zhang, F. Zhang, Q. Sui, Improved damage localization and quantification of CFRP using lamb waves and convolution neural network, *IEEE Sens. J.* 19 (14) (2019) 5784–5791.
- [38] C. Feng, H. Zhang, S. Wang, Y. Li, H. Wang, F. Yan, Structural damage detection using deep convolutional neural network and transfer learning, *KSCE J. Civ. Eng.* 23 (10) (2019) 4493–4502.
- [39] B. Zhao, C. Cheng, Z. Peng, X. Dong, G. Meng, Detecting the early damages in structures with nonlinear output frequency response functions and the CNN-LSTM model, *IEEE Trans. Instrum. Meas.* 69 (12) (2020) 9557–9567.
- [40] D. Choe, H.C. Kim, M.H. Kim, Sequence-based modeling of deep learning with LSTM and GRU networks for structural damage detection of floating offshore wind turbine blades, *Renew. Energy* 174 (2021) 218–235.
- [41] Z. Yunjie, G. Xiaorong, L. Lin, P. Yongdong, Q. Chunrong, Simulation of laser ultrasonics for detection of surface-connected rail defects, *J. Nondestr. Eval.* 36 (4) (2017), <https://doi.org/10.1007/s10921-017-0451-3>.
- [42] Y. Lecun, L. Bottou, Y. Bengio, P. Haffner, Gradient-based learning applied to document recognition[J], *Proc. IEEE* 86 (11) (1998) 2278–2324.
- [43] K. He, X. Zhang, S. Ren, J. Sun, Deep residual learning for image recognition. arXiv preprint arXiv:1512.03385 (2015).